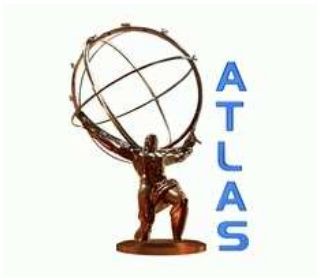

ATLAS NOTE

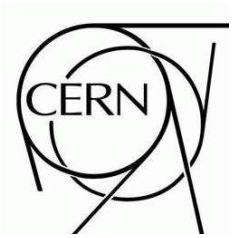

Prospects for Supersymmetry Discovery Based on Inclusive Searches

The ATLAS Collaboration[1)]

This note is part of CERN-OPEN-2008-020. This version of the note should not be cited: all citations should be to CERN-OPEN-2008-020.

ATL-PHYS-PUB-2009-066
10 May 2009

Abstract

This note describes searches for generic SUSY models with R-parity conservation in the ATLAS detector at the CERN Large Hadron Collider. SUSY particles would be produced in pairs and decay to the lightest SUSY particle, $\tilde{\chi}_1^0$, which escapes the detector, giving signatures involving jets, possible leptons, and $E_{\mathrm{T}}^{\mathrm{miss}}$. The integrated luminosity simulated is 1 fb^{-1} . This article relies on work published elsewhere in this collection, where the Standard Model backgrounds for SUSY are discussed.

[1)]This note prepared by J. Abdallah, F. Ahles, S. Asai, J. Asal, A.J. Barr, R.M. Bianchi, I. Borjanovic, J. Boyd, O.E. Brandt, P. Bruckman de Renstrom, R. Bruneliere, S. Caron, U. De Sanctis, A. De Santo, R. Di Sipio, J. Dietrich, J. Dragic, T. Eifert, A. Farbin, M. Fehling, H. Flaecher, M.H. Genest, T. Golling, B. Gjelsten, E. Gorini, S. Grancagnolo, C. Gwenlan, S. Haug, I. Hinchliffe, A. Hoecker, S. Horner, N. Kanaya, Y. Kataoka, J. Krstic, T. Lari, D. Lumb, B.R. Mellado Garcia, M. Milosavljevic, F. Paige, K. Pajchel, Y. Pan, G. Polesello, X. Portell, C. Potter, J. Poveda, M. Primavera, B.H. Samset, T. Sarangi, M. Shapiro, S. Spagnolo, J.E. Sundermann, C. Troncon S. Vahsen, J. Valls, A. Ventura N. Venturi, J. Virzi, S.L. Wu.

1 Introduction

This note describes the search for generic SUSY with R parity, so that SUSY particles are produced in pairs and decay to the lightest SUSY particle, $\tilde{\chi}_1^0$, which escapes the detector, giving signatures involving jets, possible leptons and $E_{\mathrm{T}}^{\mathrm{miss}}$, an imbalance in the transverse energy measured in the detector. Most of the introductory information necessary to the understanding of this document is given in the introductory SUSY note [1], which should be read before this one. These include a brief description of the theoretical framework, a definition of the SUSY benchmark models SUn studied in the detailed analyses, a description of the Monte Carlo samples used for signal and background. Common identification criteria for jets, taus and leptons have been adopted throughout the analyses in this note, and are also described in [1] as well as the definition of a few global variables relevant for the analysis, such as effective mass (M_{eff}), stransverse mass (m_{T2}) and transverse sphericity (S_T). The background uncertainties used throughout this work are based on Standard Model background studies documented in [2, 3]. Special signatures associated, e.g., with Gauge Mediated SUSY Breaking are treated elsewhere [4].

Two different approaches have been used to develop the inclusive search strategy described here. Firstly, detailed studies have been carried out for various signatures (jets + $E_{\mathrm{T}}^{\mathrm{miss}}$ + 0 leptons, jets + $E_{\mathrm{T}}^{\mathrm{miss}}$ + 1 lepton, ...) using data-sets fully simulated with Geant 4 for specific SUSY signal parameters and for the relevant Standard Model backgrounds. These detailed studies are used to develop deeper understanding of how best to reconstruct these relatively complex events and to define strategies for separating the signal from the Standard Model backgrounds. In order to simplify the procedure of combining the results from the different analyses, the various leptonic signatures have been defined so that they are exclusive. For example the 1-lepton signature rejects all events in which more than one lepton is present. However, no attempt is made to combine the different analyses in the present document.

Secondly, the insight gained from studying specific points has been applied to several scans over subsets of the SUSY parameter space, Since large numbers of signal points must be studied, these scans are of necessity based on fast, parameterized simulation. The goal is to verify that the different sets of basic cuts studied on benchmark points provide sensitivity to a broad range of SUSY models. The results shown in this document will be used as a basis for the development of a strategy for SUSY discovery with early ATLAS data.

1.1 Trigger

The trigger efficiency for the inclusive SUSY signals at the benchmark points has been studied based on the complete simulation of all three trigger levels of ATLAS. For all the analyses we adopted the trigger thresholds defined for 2×10^{33} cm^{-2}s^{-1} in the High Level Trigger TDR [5]. These triggers are discussed futher elsewhere [6] in this volume, where a detailed explanation of the naming convention for the trigger menu items appearing in Table 1 can be found.

The jet triggers, denoted by "JETS", consist of the logical "or" of the following triggers:

- j400: 1 jet with $p_T > 400$ GeV;
- 3j165: 3 jets with $p_T > 165$ GeV;
- 4j110: 4 jets with $p_T > 110$ GeV.

The $E_{\mathrm{T}}^{\mathrm{miss}}$ trigger "j70_xE70", requires $E_{\mathrm{T}}^{\mathrm{miss}} > 70$ GeV accompanied by a jet with $p_T > 70$ GeV. The lepton triggers are "e22i": an isolated electron efficient for $p_T > 25$ GeV; "2e12i": two isolated electrons efficient for $p_T > 15$ GeV, "mu20": a muon with $p_T > 20$ GeV and "2mu10": two muons with $p_T > 10$ GeV.

Table 1: Average event trigger efficiency (in %) for events passing various lepton and jet selection criteria described in detail in the indicated sections.

Trigger	SU1	SU2	SU3	SU4	SU6	SU8.1
	0-lepton, 4-jet selection [Section 2.1]					
JETS	44.6	51.0	33.8	7.7	51.7	48.2
j70_xE70	99.7	98.7	99.5	97.2	99.6	99.7
	0-lepton, 3-jet selection [Section 2.2]					
JETS	64.9	71.1	54.9	34.3	71.8	66.8
j70_xE70	100.	99.8	100.	99.9	100.	100.
	0-lepton, 2-jet selection [Section 2.2]					
JETS	44.1	39.9	30.1	8.8	53.6	47.6
j70_xE70	100.	100.	100.	99.9	100.	100.
	1-lepton, selection [Section 3]					
JETS	41.8	50.5	31.7	8.1	48.4	45.6
j70_xE70	99.6	99.0	98.9	95.6	98.9	99.1
1LEP (mu20 OR e22i)	81.2	81.0	79.9	80.3	80.4	79.5
	OS 2-lepton, selection [Section 4.1]					
JETS	36.7	47.3	34.0	6.7	47.2	40.8
j70_xE70	99.2	100.0	98.9	94.3	99.6	100.0
1LEP (mu20 OR e22i)	87.0	90.0	87.5	84.8	79.6	86.4
2LEP (2mu10 OR 2e15i)	20.5	35.5	27.0	18.0	26.0	14.6
	SS 2-lepton, selection [Section 4.2]					
JETS	39.9	48.8	29.2	1.6	46.6	34.5
j70_xE70	99.3	100.0	98.9	84.1	98.3	100.0
1LEP (mu20 OR e22i)	94.2	92.7	95.9	95.2	89.7	96.6
2LEP (2mu10 OR 2e15i)	32.6	41.5	32.2	25.4	25.9	31.0
	3-lepton, selection [Section 5]					
JETS	43.7	60.2	40.1	17.6	46.4	48.3
j70_xE70	95.6	85.4	93.5	79.8	96.4	98.3
1LEP (mu20 OR e22i)	95.2	94.2	95.8	94.7	94.6	96.7
2LEP (2mu10 OR 2e15i)	49.1	60.2	51.0	44.7	47.3	53.3

Since the goal of this note is to develop a generic SUSY search, only the basic trigger building blocks have been considered. More complex triggers combining different objects can be easily implemented in the trigger menus. Also, only triggers which are not prescaled have been used.

The trigger efficiencies for the signal events passing the the 0, 1, 2, and 3-lepton selections defined in the following sections are listed in Table 1 for different requirements on jet multiplicity. In general the j70_xE70 is highly efficient, although there is some loss for SU4, the low-mass point with a very large cross-section. The j70_xE70 trigger is also very efficient for the τ and b modes, described in Sections 6 and 7 below.

The basic performance of the leptonic and j70_xE70 triggers will be determined from Standard Model events such as Z and $\bar{t}t$ using the methods described in [6]. It may be useful to check that performance by comparing (Monte Carlo) samples of SUSY events selected with multiple triggers. For the 0-lepton selection, the efficiency for JETS trigger alone is in the range 30-70%, except for the very low mass point SU4. This provides a useful redundancy in the early phases, as the $E_{\mathrm{T}}^{\mathrm{miss}}$ trigger may require a longer time

than the other triggers to be completely understood, but only j70_xE70 has an efficiency close to one. For the topologies involving leptons, both the single lepton triggers and j70_xE70 have typical efficiencies in excess of 80%, so comparing them should be quite effective.

1.2 Systematic uncertainties and statistical procedure

To assess the discovery potential of the different analyses it is necessary to take into account systematic uncertainties. SUSY searches will address very complex topologies, typically with many jets in the final state. The prediction of the Standard Model backgrounds to these topologies will require a complex interplay of Monte Carlo and data-driven methods. The development of these methods and the estimate of the corresponding uncertainties are described in detail in [2] and [3]. The approximate uncertainties for an integrated luminosity of $1\,\text{fb}^{-1}$ are estimated to be:

- 50% for the background from QCD multijet events,
- 20% for the background from $t\bar{t}$, $W+$jets, $Z+$jets, and W/Z pairs.

The limited Monte Carlo statistics is also taken into account and all systematic uncertainties are added in quadrature. The background can never be known exactly. Uncertainties on the background are incorporated in the significance by convoluting the Poisson probability that the background fluctuates to the observed signal with a Gaussian background probability density function with mean N_b and standard deviation δN_b (see e.g. [7,8] and references therein). Given these assumptions, the probability p that the background fluctuates by chance to the measured value N_{data} or above is given by

$$p = A \int_0^\infty db\; G(b; N_b, \delta N_b) \sum_{i=N_{\text{data}}}^{\infty} \frac{e^{-b} b^i}{i!},$$

where $G(b; N_b, \delta N_b)$ is a Gaussian and the factor

$$A = \left[\int_0^\infty db\; G(b; N_b, \delta N_b) \sum_{i=0}^{\infty} e^{-b} b^i / i! \right]^{-1}$$

ensures that the function is normalised to unity. If the Gaussian probability density function G is replaced by a Dirac delta function $\delta(b - N_b)$, the estimator p results in a usual Poisson probability.

The probability p is transformed into "standard-deviations", denoted in this note by the symbol Z_n, using the formula

$$Z_n = \sqrt{2}\,\text{erf}^{-1}(1 - 2\text{p})$$

The Root [9] library provides functions to calculate p and Z_n.

If many different data selections are considered, it becomes more likely that statistical fluctuations would be misinterpreted as new phenomena if the number of selections is not considered in the statistical procedure. This is known in statistics as the problem of "multiple comparisons". The probability values are therefore corrected for multiple comparisons via a Monte Carlo method. The effect is the reduction of approximately half a unit of Z_n for $Z_n = 3$, decreasing with increasing Z_n. In the last section of the note the significance always corresponds to the corrected Z_n.

2 Zero-lepton mode

A SUSY signal at the LHC is typically dominated by the production of squarks and gluinos. In the R-parity conserving case, at the end of each sparticle decay chain one finds an undetected LSPs, which

Table 2: Number of events surviving subsequent selection cuts as defined in the text for 4-jets analysis normalized to 1fb^{-1} using NLO cross-sections.

Sample	Cut 1	Cut 2	Cut 3	Cut 4	Cut 5	M_{eff} Cut
SU3	9600	7563	5600	5277	4311	3349
SU1	3485	2854	2004	1907	1401	1229
SU2	604	369	308	279	169	131
SU4	79618	57803	46189	42408	34966	8507
SU6	2551	2062	1468	1383	1080	956
SU8.1	3118	2540	1778	1686	1448	1284
MC@NLO $t\bar{t}$	12861	8798	6421	5790	4012	305
Pythia QCD	29230	7044	4667	848	848	13
Alpgen Z	1626	1045	732	660	644	162
Alpgen W	4066	2393	1654	1499	1147	228
Herwig WZ	22	15	9	8	4	1
Total Standard Model	47805	19294	13483	8806	6655	708
SU3 S/B	0.2	0.4	0.4	0.6	0.6	4.7
Z_n	0.5	1.3	1.4	2.6	2.7	13
SU3 eff (excl)	35.1%	78.8%	74.0%	94.2%	81.7%	77.9%
SU3 eff (incl)	35.1%	27.7%	20.5%	19.3%	15.8%	12.3%

can together generate large $E_{\text{T}}^{\text{miss}}$. The least model-dependent SUSY signature is therefore the search for events with multiple jets and $E_{\text{T}}^{\text{miss}}$. Traditionally searches have been performed requiring at least four jets; the high multiplicity helps to reduce the background from QCD and $W/Z+$jets. Both for this topology and for the leptonic topologies in the following sections we adopt very simple sets of cuts, similar to the ones used in the ATLAS Physics TDR [10]. In addition to the four-jet signatures we have also addressed signatures with lower jet multiplicity. These signatures have more backgrounds, but might be favoured in some SUSY models, and should be more cleanly reconstructed in the detector, because of their less-complex topologies. This may be an advantage in the early phases of the experiment.

2.1 Four or more jets in final state

The basic selections applied for this channel are:

1. At least four jets with $p_T > 50$ GeV at least one of which must have $p_T > 100$ GeV; and $E_{\text{T}}^{\text{miss}} > 100$ GeV.
2. $E_{\text{T}}^{\text{miss}} > 0.2 M_{\text{eff}}$.
3. Transverse sphericity, $S_T > 0.2$.
4. $\Delta\phi(\text{jet}_1 - E_{\text{T}}^{\text{miss}}) > 0.2$, $\Delta\phi(\text{jet}_2 - E_{\text{T}}^{\text{miss}}) > 0.2$, $\Delta\phi(\text{jet}_3 - E_{\text{T}}^{\text{miss}}) > 0.2$.
5. Reject events with an e or a μ.
6. $M_{\text{eff}} > 800$ GeV.

Most of the background samples have been filtered at generation level with various requirements on $E_{\text{T}}^{\text{miss}}$ and jet multiplicity. The first cut in the analysis flow applies harder requirements than any of the ones applied at the filter level to minimise the bias to the study from the use of filtered samples.

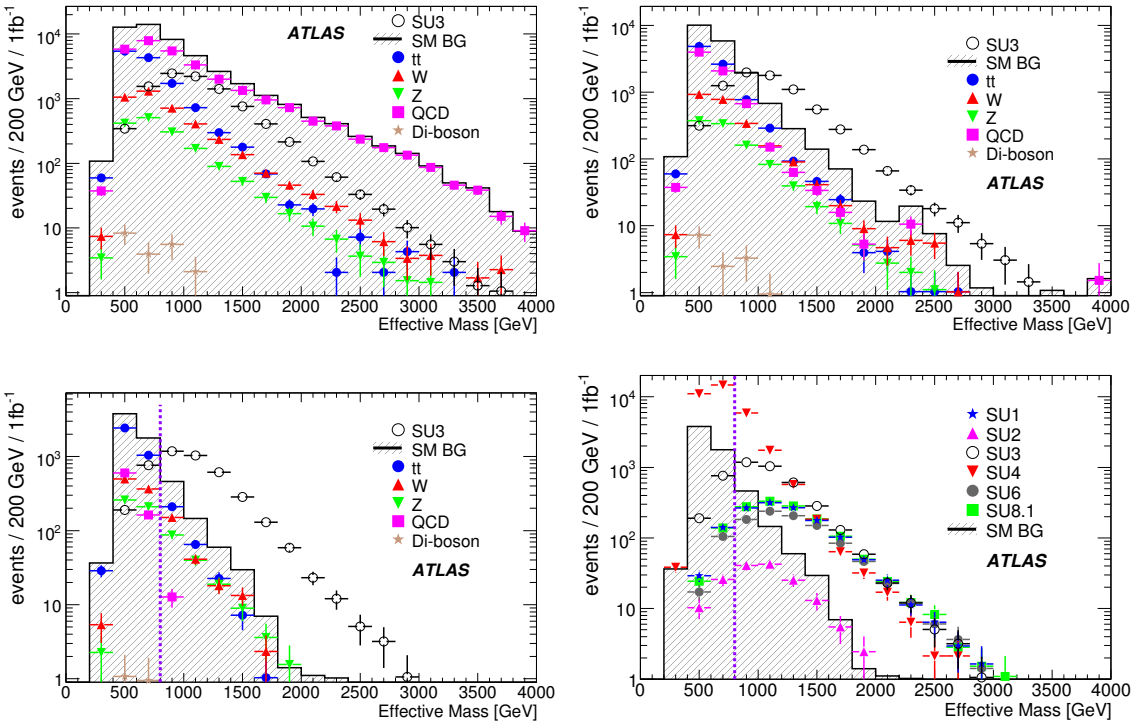

Figure 1: M_{eff} distribution for events surviving successive selection cuts: cut 1 (top left), cut 2 (top right), and cuts 3-5 (bottom left). The open circles represent point SU3, and the different background contributions are shown according to the legend. The last plot (bottom right) show all of the SUSY benchmark points and the total Standard Model background after cuts 1-5. Open circles represent the SUSY SU3 signal as predicted by Monte Carlo simulation, while the shaded area shows the total Standard Model background.

The main background at this point from QCD events where $E_{\text{T}}^{\text{miss}}$ is produced either by a fluctuation in the measurement of the energy of one or more jets, or by a real neutrino from the decay of a B hadron produced in the fragmentation process. Since the statistical fluctuation on the $E_{\text{T}}^{\text{miss}}$ measurement grow with increasing M_{eff}, the second cut above eliminates the Gaussian part of the $E_{\text{T}}^{\text{miss}}$ measurement fluctuations. In SUSY events the jets are produced from the decay of heavy particles produced approximately at rest, and are thence distributed isotropically in space, whereas for the QCD events the direction of the two partons from the hard scattering provides a privileged direction. The cut on sphericity is intended to exploit this fact. Both for jet mismeasurement and for b decays, the $E_{\text{T}}^{\text{miss}}$ vector will be close the direction of one jets, and so the $\Delta\phi$ cuts are very efficient in reducing the QCD background. The lepton veto is applied in order to facilitate the combination with analyses requiring leptons, but it is not expected to significantly modify the signal-to-background ratio.

The number of events surviving each of the cuts for an integrated luminosity of $1\,\text{fb}^{-1}$ is shown in Table 2 for all of the considered benchmark points and for the backgrounds. The number of events in the last column includes the effect of the j70xE70 trigger, which, as shown in Table 1, has an efficiency in excess of 97% for all considered signal benchmarks.

The distribution of the final selection variable M_{eff}, for signal and background, is shown in Fig. 1 for point SU3 at different stages of the analysis. The QCD background is dominant after the first cut but is reduced to a similar level to the backgrounds containing real neutrinos by subsequently requiring

$E_{\mathrm{T}}^{\mathrm{miss}} > 0.2 M_{\mathrm{eff}}$ (cut 2). The cuts on event sphericity and $\Delta\phi$ strongly reduce the QCD background, which becomes concentrated in the region of low M_{eff}. After all cuts $t\bar{t}$ is the dominant background, but there are also significant contributions from $W+$jets and $Z+$jets. The final cut, $M_{\mathrm{eff}} > 800$ GeV, reduces the background to below the level of the signal for all considered benchmark points except for SU2. For this point to be found in the 0-lepton channel, one would have to select larger values of M_{eff} to enhance the signal-to-background ratio, and a greater integrated luminosity would be required.

The statistical significance Z_n for $1\,\mathrm{fb}^{-1}$ was calculated using the prescription in Section 1.2 including the systematic uncertainty on the background [2, 3]. The significance for point SU3 after each cut is shown in Table 2. The significances Z_n after all cuts are 13 for SU3, 6.3 for SU1, 0.9 for SU2, 25 for SU4, 6.3 for SU6, and 6.5 for SU8.1. Evidently only point SU2, for which the cross section is dominated by direct gaugino production (which is investigated elsewhere in this volume [11]), would not be accessible for the assumed set of cuts, integrated luminosity and level of background understanding.

These numbers should be taken as indicative. The uncertainty on the background used in the calculation is the estimate of what one would obtain using complicated procedures for background evaluation based on a combination of data-driven and Monte Carlo methods. The absolute value of the backgrounds used for this study is derived only from Monte Carlo, and the present uncertainty on this value is much higher. An idea of the robustness of the analysis can be obtained by studying the significance for the benchmark points if the background would be increased by a factor 2. In this case the significance for SU3 would drop to 7.8, and the one for SU6 to approximately 3.1. The significance for SU6 would be, in this situation, dominated by the systematic uncertainty on the background evaluation. Therefore an increase in integrated luminosity would result in an increased reach only if it can be used to reduce the uncertainty on the background evaluation.

2.2 Inclusive two-jet and three-jet final states

The analyses based on lower jet-multiplicities are based on very similar requirements to the 4-jet analysis above. The differences are: higher p_{T} requirements on the remaining jets to cope with the increased QCD background, and a slightly harder $E_{\mathrm{T}}^{\mathrm{miss}}$ cut. The sphericity cut is less relevant in the case of low jet multiplicities and is dropped. For the two (three)-jet analysis the cuts are respectively:

1. At least two (three) jets, the hardest with $p_T > 150$ GeV and the second (and third) with $p_T > 100$ GeV; $E_{\mathrm{T}}^{\mathrm{miss}} > 100$ GeV
2. $E_{\mathrm{T}}^{\mathrm{miss}} > 0.3(0.25) M_{\mathrm{eff}}$.
3. $\Delta\phi(\mathrm{jet}_1 - E_{\mathrm{T}}^{\mathrm{miss}}) > 0.2$, $\Delta\phi(\mathrm{jet}_2 - E_{\mathrm{T}}^{\mathrm{miss}}) > 0.2$, $(\Delta\phi(\mathrm{jet}_3 - E_{\mathrm{T}}^{\mathrm{miss}}) > 0.2)$
4. Reject events with an e or a μ
5. $M_{\mathrm{eff}} > 800$ GeV.

The M_{eff} variable is different from the one defined in [1] in that only the 2(3) highest p_{T} jets for the 2–(3–)jet analysis are used.

Since the ALPGEN $W+$jets and $Z+$jets background samples have a filter at generation level requiring 4 jets, samples produced with the PYTHIA generator were used in this case.

The cut flow for the 2-jet analysis is given in Table 3, and the M_{eff} distributions before the M_{eff} cut for the different background contributions and for the different signal points are shown in Figure 2. The number of events after all cuts includes the effect of the j70xE70 trigger, which, as shown in Table 1, has an efficiency in excess of 99% for all considered SUSY benchmark points. After the $\Delta\phi$ cuts the $t\bar{t}$, $W+$jets, $Z+$jets and QCD all give comparable contributions to the background. After all cuts the surviving events are approximately doubled both for signal and background, as compared to the 4-jet

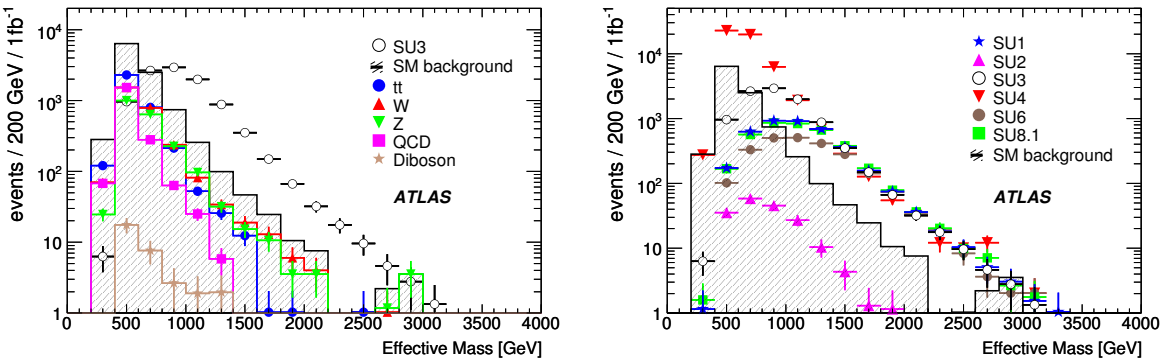

Figure 2: M_{eff} distribution for the 0-lepton plus 2-jet analysis, after final cuts. Left: The open circles show the SUSY (SU3) signal Monte Carlo prediction, while the total Standard Model background is shown by the shaded histogram. The individual background contributions are shown by the points, as described in the legend. Right: The points show the distribution of the signal for a number of SUn points.

Table 3: Number of events surviving the selection cuts defined in the text for the 2–jet analysis. Entries are normalized to 1 fb^{-1} using next-to-leading-order cross-sections.

Sample	Cut 1	Cut 2	Cut 3	Cut 4	M_{eff} Cut
SU3	18660.7	12519.8	12217.5	10055.2	6432.2
SU1	7699.9	5427.5	5318.1	3996.8	3196.0
SU2	642.4	319.7	301.2	185.1	90.4
SU4	123219	64502.4	62172.9	52108.0	9434.4
SU6	4483.1	3133.5	3041.7	2418.5	1987.0
SU8.1	6384.7	4482.5	4381.8	3804.5	3067.7
$t\bar{t}$	17666.6	6273.8	5778.6	3556.7	304.8
QCD	124513.9	7341.7	1983.7	1983.7	107.6
$Z+$jets	3222.5	2192.2	2109.5	2056.1	391.6
$W+$jets	8887.2	4504.5	4072.4	2775.5	395.1
Diboson	150.4	71.2	66.0	32.1	6.8
Standard Model	154440.5	20383.4	14010.1	10404.1	1205.8
SU3 S/B	0.12	0.61	0.87	0.97	5.3
SU3 $S/\sqrt{B}$	47.5	87.7	103.2	98.6	185.2
SU3 eff (cum)	67.4%	45.2%	44.1%	36.3%	23.2%
SU3 eff (excl)	67.4%	67.1%	97.6%	82.3%	64.0%

analysis, except for the low-mass SU4 points for which the harder kinematic cuts reduce the signal efficiency.

Assuming the estimated systematic background errors are the same as for the 4–jet case, the estimated significances are 13.3 for SU3, 8.0 for SU1, 17.2 for SU4, 5.5 for SU6, and 7.7 for SU8.1, for 1 fb^{-1} of integrated luminosity. The significance for SU2, for which direct gaugino production is dominant, is less than 1.0. The equivalent numbers for the 3–jet analysis are: 17.0 for SU3, 9.5 for SU1, 25.7 for SU4, 7.3 for SU6 and 9.6 for SU8. Although the signal over background ratio is equivalent or better (for

the three-jet topology) than for the 4-jet analysis this is only partially reflected in the significances when the systematic uncertainty is taken into account. This is due to the increased contribution of the QCD background, which has an estimated uncertainty on QCD is of 50%, as compared to 20% for the other backgrounds. Therefore, since the uncertainties of the backgrounds were evaluated for a 4-jet analysis, a dedicated background study would be needed to obtain a correct estimate of the discovery potential in this topology.

The 2-, 3- and 4-jet analyses are based on very similar cuts and therefore have a large overlap in the selected events. About 40% of all 2-jet events are also contained in the 3-jet slection and about 35% in the 4-jet selection. The biggest overlap is for the 3 jet events: about 59% of all 3-jet events are also contained in the 4-jet analysis and about 97% in the 2-jet analysis.

An alternative strategy was explored where cuts 2 and 3 of the M_{eff} analysis are dropped, and a cut on the m_{T2} variable [12, 13], $m_{T2} > 400$ GeV, is applied as the only discriminating observable. The m_{T2} variable, has the interesting properties that it takes low values for events where either the visible p_T or $E_{\text{T}}^{\text{miss}}$ are small, and in the case of small $\Delta\phi$. It can therefore replace these topological cuts. For semi-invisibly decaying particles m_{T2} is related to the difference in mass between the particles produced in the interactions and their invisible decay products. It can therefore take a larger value for SUSY events than for top or W events. Taking the estimates of the systematic background errors into account, the significances for the 2-jet m_{T2} analysis are: 15.6 for SU3, 11.5 for SU1, 10.9 for SU4, 8.3 for SU6, and 11.1 for SU8.1, somewhat better than the equivalent analysis based on M_{eff}. The most effective strategy will be ultimately defined by how well the systematic uncertainty on the background evaluation can be controlled in the different approaches.

3 One-lepton mode

While the 0-lepton mode with multiple jets plus $E_{\text{T}}^{\text{miss}}$ is probably the most generic search mode for SUSY with R-parity conservation, it is sensitive to backgrounds from mismeasured QCD multijet events. Requiring one lepton in addition to multiple jets and $E_{\text{T}}^{\text{miss}}$ greatly reduces the potential QCD multijet background; the remaining backgrounds are under better control. Even if τ decays of gauginos are dominant, leptonic τ decays provide a significant 1-lepton rate, at least for high masses. It is not surprising, therefore, that the reach in the 1-lepton and 0-lepton modes are comparable.

The cuts in this analysis are similar to those used in the ATLAS Physics TDR [10] but also include a cut on the transverse mass[2)], M_T, formed from the lepton and $E_{\text{T}}^{\text{miss}}$ which has the role of suppressing the $W+$jets and $t\bar{t}$ backgrounds. The S_T cut is included for historical reasons, but its effectiveness is questionable:

1. Exactly one isolated lepton with $p_T > 20$ GeV satisfying the selection criteria described earlier.
2. No additional leptons with $p_T > 10$ GeV. This ensures no overlap with the 0-lepton, 2-lepton, and 3-lepton analyses.
3. At least four jets with $p_T > 50$ GeV at least one of which must have $p_T > 100$ GeV.
4. $E_{\text{T}}^{\text{miss}} > 100$ GeV and $E_{\text{T}}^{\text{miss}} > 0.2 M_{\text{eff}}$.
5. Transverse sphericity, $S_T > 0.2$.
6. Transverse mass, $M_T > 100$ GeV.

[2)] Note the distinction between the transverse mass, M_T, which is a function of the momentum of one visible particle and the missing transverse momentum and the *stransverse* mass which is a function of the momenta of two visible particles and the missing transverse momentum.

Table 4: Number of events surviving the selection cuts defined in the text for the 1-lepton analysis. Entries are normalized to 1 fb^{-1} using NLO cross-sections. The last column reports a simple $S/\sqrt{B}$ calculation of the corresponding significance of an observation for the SUSY benchmark points (SUn).

Sample	Cuts 1–4	Cut 5	Cut 6	Cut 7	$S/\sqrt{B}$
SU1	571.7	423.0	259.9	232.3	36.0
SU2	86.7	75.6	46.1	39.6	6.1
SU3	995.7	767.9	450.5	363.6	56.4
SU4	7523.6	6260.4	2974.4	895.8	138.9
SU6	342.3	250.9	161.9	147.9	22.9
SU8.1	296.4	214.4	151.4	136.3	21.1
$t\bar{t}$	2028.5	1546.8	131.7	36.0	
W	425.2	314.8	9.9	5.4	
Z	39.0	27.3	1.7	0.2	
Diboson	7.3	5.1	0.8	0.0	
QCD	0.0	0.0	0.0	0.0	
Standard Model BG	2500.1	1894.0	144.1	41.6	

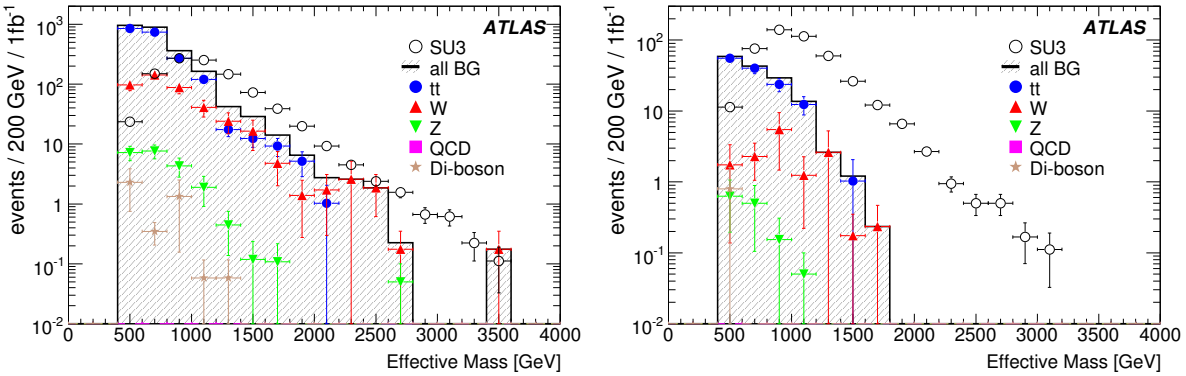

Figure 3: Expected M_{eff} distributions after Cuts 1–4 (left), and Cut 6 (right) for the 1-lepton analysis. Compare with Table 4.

7. $M_{\text{eff}} > 800$ GeV.

Cuts 1–2 define the 1-lepton analysis, while Cuts 3–4 both reduce the Standard Model backgrounds and ensure compatability with the Standard Model filter cuts. Distributions without these four cuts are not meaningful and so are not shown. Cut 5 reduces the $E_{\text{T}}^{\text{miss}}$ background from mismeasured dijet events; Cut 6 reduces the background from events in which the $E_{\text{T}}^{\text{miss}}$ comes from $W \to \ell\nu$; and Cut 7 selects high-mass final states.

The cut flow table for these cuts is shown in Table 4. The number of events after all cuts includes the effect of the j70xE70 trigger, which, as shown in Table 1, has an efficiency of around 99% for all the benchmark points considered other than the low mass SU4 point, for which the efficiency is still above 95%. Note that the QCD background is reduced to a negligible level by the lepton and $E_{\text{T}}^{\text{miss}}$ cuts as expected. The background after all cuts is dominated by $t\bar{t}$ and $W+$jets, both of which are expected to be better understood than the QCD background. Therefore, while the 1-lepton mode may not have better reach than the 0-lepton mode given the calculated backgrounds, its reach seems more robust against

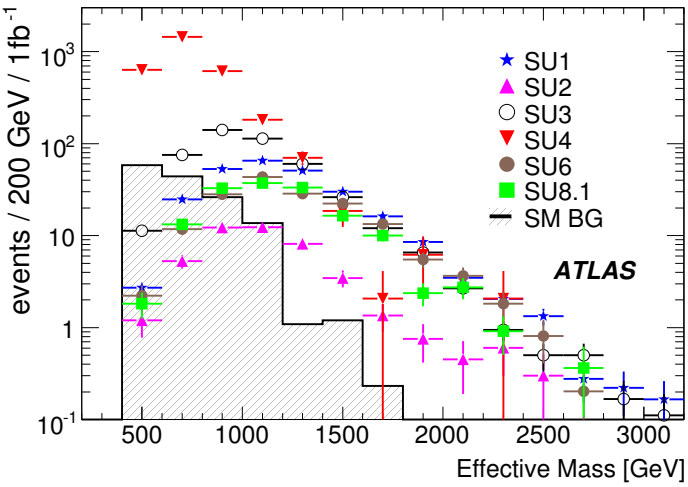

Figure 4: The M_{eff} distributions for each of the SUn benchmark points, and for the sum of the Standard Model backgrounds with $1\,\text{fb}^{-1}$ for the 1-lepton analysis. All the cuts except on M_{eff} are applied.

Table 5: Significance Z_n for the 1-lepton plus 4-jet analysis with $1\,\text{fb}^{-1}$ including the systematic uncertainty in the background estimation.

Sample	$M_{\text{eff}} > 400$ GeV		$M_{\text{eff}} > 800$ GeV		$M_{\text{eff}} > 1200$ GeV	
	Events	Z_n	Events	Z_n	Events	Z_n
Standard Model BG	144		42		2	
SU1	260	7.6	232	12.3	114	18.0
SU2	46	1.5	40	3.4	15	6.0
SU3	450	9.5	364	16.7	110	17.7
SU4	2974	33.7	896	29.4	99	16.6
SU6	162	4.9	148	8.9	76	14.2
SU8.1	151	4.6	136	8.4	66	13.1

background uncertainties.

The M_{eff} distribution for point SU3 after each cut is shown in Figure 3. The $E_{\text{T}}^{\text{miss}}$ and M_{eff} distributions for all the SUn points after all cuts are shown in Figures 4. It is clear from these figures and from Table 4 that the only significant backgrounds to the 1-lepton mode are from $t\bar{t}$ and $W+$jets, as one would expect. The estimated error on both of these backgrounds using data-driven methods is $\pm 20\%$ [2]. Given this and the calculated signal and background rates in Table 4, it is evident that all the SUSY points considered except SU2 could be discovered with good significance in the 1-lepton mode. For SU2, the production cross-section is dominated by gaugino pair production, so a different analysis [11] is required.

To make this conclusion more quantitative, the significance Z_n defined in Section 1.2 was calculated. The central value of each background is taken from the current Monte Carlo simulation; the studies of data-driven background estimation [2, 3] provide estimated errors of $\pm 50\%$ for QCD multijet backgrounds and $\pm 20\%$ for $t\bar{t}$, $W+$jets, and all other backgrounds. The results of this calculation are shown in Table 5 for an integrated luminosity of $1\,\text{fb}^{-1}$. Each of these points except SU2 would have $Z_n > 5$ for just $100\,\text{pb}^{-1}$ if the same 20% background uncertainty could be obtained with that luminosity.

The significances, Z_n, (Table 5) for $1\,\text{fb}^{-1}$ are much smaller than the $S/\sqrt{B}$ values in Table 4. This reflects the fact that, unlike $S/\sqrt{B}$, the Z_n measure of significance includes the estimated systematic

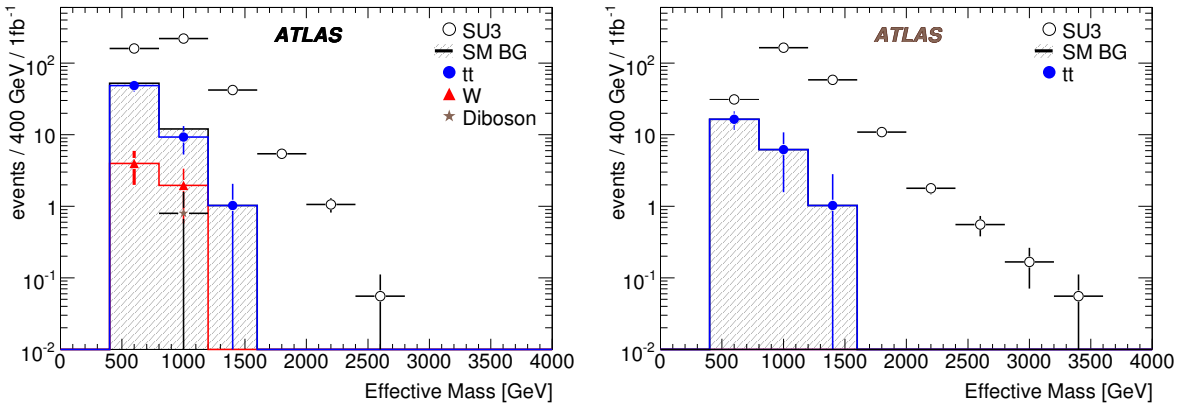

Figure 5: M_{eff} distribution for events with one lepton and: 2 jets (left) or 3 jets (right) after all cuts were applied.

uncertainty on the background. Table 5 also indicates that, provided the relative uncertainties in the background determiations did note increase, harder M_{eff} cuts would lead to better significances after systematic uncertainties in the background are taken into account.

Supersymmetry events need not contain large numbers of jets. For example, in mSUGRA the process

$$\begin{aligned} \tilde{q}_L + \tilde{q}_R \rightarrow & \tilde{\chi}_1^{\pm} q' + \tilde{\chi}_1^0 q \\ & \hookrightarrow \tilde{\chi}_1^0 \ell^{\pm} \nu \end{aligned}$$

can have a large rate and gives one lepton and just two hard jets. An alternative 1-lepton analysis has been performed requiring just two or three jets rather than four. Because a 4-jet selection was applied to the Alpgen samples at the generator level, Pythia was used for the $W+$jets backgrounds. The jet cuts employed are harder: 150 GeV for the leading jet and 100 GeV for the others. The missing energy cut is also harder, $E_{\text{T}}^{\text{miss}} > \max(100\text{ GeV}, 0.3M_{\text{eff}})$ and $\max(100\text{ GeV}, 0.25M_{\text{eff}})$ for the 2-jet and 3-jet case respectively. The M_{eff} distributions after all cuts are shown in Figure 5. Evidently an analysis requiring a smaller number of jets with harder cuts also can be effective.

4 Two-lepton mode

4.1 Opposite sign dileptons

Supersymmetry events with two opposite-sign leptons can arise from neutralino decays, especially $\chi_2^0 \rightarrow l^{\pm} l^{\mp} \chi_1^0$, either directly or through an intermediate slepton. Such dileptons must have the same flavour to avoid inducing $\mu \rightarrow e\gamma$ and other lepton-flavour-violating interactions at one loop. By contrast leptons produced from independent decays can give either same-flavour (OSSF) or different-flavour (OSDF) dilepton pairs, again with $\ell \in \{e, \mu\}$.

The opposite-sign dilepton analysis uses the following cuts:

1. Two isolated, opposite-sign leptons with $p_T > 10$ GeV and $|\eta| < 2.5$ which satisfy the cuts described in the introductory SUSY note [1]. Events containing additional leptons were vetoed.

2. At least four jets with $p_T > 50$ GeV at least one of which must have $p_T > 100$ GeV.

Table 6: The number of events surviving the selection cuts defined in the text for the opposite-sign dilepton analysis, normalized to 1fb^{-1} using next-to-leading-order cross-sections. The last two columns give the S/B ratio and the Z_n significance, the latter of which includes the systematic uncertainties on the Standard Model backgrounds.

Sample	Cuts 1-3	Cut 4	S/B	Z_n
SU3	200.8	159.8	1.88	3.55
SU1	91.0	72.6	0.86	1.65
SU2	22.5	18.8	0.22	0.43
SU4	948.0	809.5	9.56	22.5
$t\bar{t}$	111.1	81.5		
$W+$jets	2.47	1.97		
$Z+$jets	1.77	1.20		
QCD (J3-J7)	0	0		
Total Standard Model	115.34	84.67		

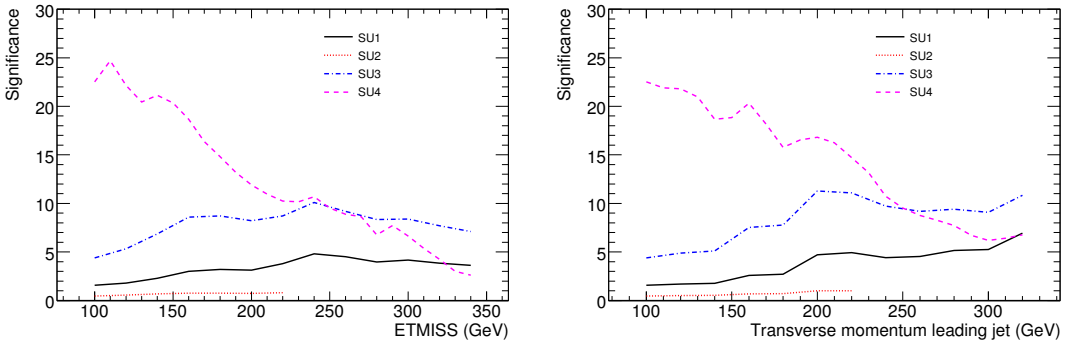

Figure 6: Significance of signal events for the four benchmark points, as a function of the cut on transverse missing energy (left) and the transverse momentum of the leading jet (right), for an integrated luminosity of $1\,\text{fb}^{-1}$.

3. $E_{\text{T}}^{\text{miss}} > 100$ GeV and $E_{\text{T}}^{\text{miss}} > 0.2 M_{\text{eff}}$.

4. Transverse sphericity, $S_T > 0.2$.

Cut 1 defines the opposite-sign dilepton sample, while Cuts 2 and 3 both suppress the Standard Model backgrounds and provide consistency with the Monte Carlo generator cuts on those backgrounds. After Cuts 1–3 the dominant background by far is $t\bar{t}$, as one would expect. The S_T cut only increases the S/B ratio by about 8% while reducing the signal by 20%.

The signals and backgrounds after the cuts, and the corresponding significances, are shown in Table 6. The number of events after all cuts includes the effect of the j70xE70 trigger, which, as shown in Table 1, has an efficiency of around 99% for all considered signal benchmarks, except for the low mass SU4 point, for which the efficiency is above 95%. The benchmark points SU3 and SU4 both have high discovery potential in the dilepton channel. While SU1 has fairly large dilepton branching ratios, many of the leptons are soft because of the small mass gaps between supersymmetric particles. An improved analysis based low-p_T lepton reconstruction algorithms would help greatly for this point.

It is instructive to see how the significances, Z_n, vary with the cut on the leading jet and on $E_{\text{T}}^{\text{miss}}$. This is shown in Figure 6 for each of the points SU1 – SU4. It can be seen that the significance improves with

Table 7: The optimized cuts for each point and corresponding signal, background, and significance. Compare with Table 6.

Sample	$E_{\rm T}^{\rm miss}$ cut	Leading jet cut	signal	background	Significance
SU1	100 GeV	320 GeV	37.97	6.30	6.94
SU2	140 GeV	200 GeV	13.74	22.68	1.07
SU3	140 GeV	200 GeV	125.34	22.68	11.45
SU4	110 GeV	100 GeV	772.53	66.80	24.70

Table 8: The number of OSSF and OSDF dilepton events passing the optimized cuts and the corresponding statistical significance for $1\,{\rm fb}^{-1}$.

Sample	$E_{\rm T}^{\rm miss}$ cut	Leading jet cut	N_{OSSF}	N_{OSDF}	Significance
SU1	220 GeV	100 GeV	90.69	58.53	2.63
SU2	140 GeV	100 GeV	31.64	29.95	0.22
SU3	160 GeV	160 GeV	93.75	38.58	4.80
SU4	120 GeV	100 GeV	392.45	281.55	4.27

harder cuts than those given in the above cut list even for the low-mass point SU4. The optimal cuts for each point and the signal, background and significance are shown in Table 7. Systematic errors of 50% on on all Standard Model backgrounds are included. Of course one should not optimize an analysis for a single point, but the table suggests that, provided the systematic uncertainties on the Standard Model background determinations do not significantly increase, harder cuts would be preferred. Optimization for wider ranges of points is discussed in Section 8.

Observing an non-resonant excess of OSSF dilepton events over OSDF events would be a clear indication of new physics. In SUSY leptonic $\tilde{\chi}_2^0$ decays can produce this excess, and have a characteristic endpoint set by the masses involved. The significance of the difference, calculated as $(N_{OSSF} - N_{OSDF})/\sqrt{N_{OSSF} + N_{OSDF}}$, is shown in Table 8. This significance calculation assumes that the relative e and μ acceptances are well understood, which is not unreasonable given that all Standard Model processes satisfy $e/\mu/\tau$ universality. For SU1 the combined branching ratio for $\tilde{\chi}_2^0 \to \tilde{\ell}_{L,R}^{\pm}\ell^{\mp}$ is 11.7%, but the acceptance is reduced by the small mass gaps. For SU2 gaugino pair production dominates, so the jet cuts suppress the signal.

4.2 Same sign dileptons

In the Standard Model the rate for prompt, isolated, same-sign dileptons is small. Of course some leptons from hadronized heavy or light quarks can also pass the isolation cut and contribute like-sign backgrounds. In SUSY, on the other hand, the gluino is a self-conjugate Majorana fermion, so events containing like-sign dileptons can be common. Thus, same-sign dileptons are a good signature for SUSY and a characteristic feature of it.

The cuts used for the same-sign dilepton analysis are:

1. Exactly 2 same-sign leptons with $p_T > 20$ GeV satisfying the usual isolation and other cuts [1].
2. At least four jets with $p_T > 50$ GeV at least one of which must have $p_T > 100$ GeV.
3. Transverse missing energy $E_{\rm T}^{\rm miss} > 100$ GeV.

Table 9: The number of events surviving the selection cuts (as defined in the text) for the same-sign dileptons analysis, normalized to 1fb^{-1} using next-to-leading-order cross-sections. No background events pass the final cut; the 90% upper limit for $t\bar{t}$ background is given.

Process	Cuts 1–3	Cut 4	Z_n
SU1	30.1	21.9	7.2
SU2	13.0	6.6	1.9
SU3	37.9	24.9	7.7
SU4	251.8	138.8	19.9
SU6	18.0	13.9	4.5
$t\bar{t}$	2.1	< 2.3	
$W+$jets	0.7	0.0	
$Z+$jets	0.0	0.0	

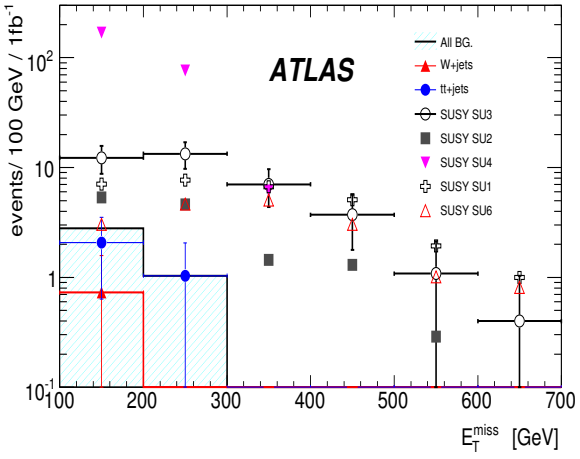

Figure 7: $E_{\mathrm{T}}^{\mathrm{miss}}$ in the same sign dilepton events after all cuts except the $E_{\mathrm{T}}^{\mathrm{miss}}$ cut.

4. $E_{\mathrm{T}}^{\mathrm{miss}} > 0.2 M_{\mathrm{eff}}$.

The first cut defines the same-sign dilepton sample, while Cuts 2-4 suppress the Standard Model backgrounds. Cuts 1 and 2 are used in the Monte Carlo generator filters for some of the backgrounds.

The cut flow table for these cuts is shown in Table 9. The number of events after all cuts includes the effect of the j70xE70 trigger, which, as shown in Table 1, has an efficiency of around 99% for all considered signal benchmarks, except for the low mass SU4 point, for which the efficiency is 84%.

Since the $W+$jets and $Z+$jets backgrounds have been filtered at the generator level, the results for these are biased until after Cut 3, but evidently they are small. A number of other backgrounds were examined and found to be negligible compared to those listed in the table. None of the Monte Carlo events generated for the Standard Model background determination passed all the cuts. A 90% confidence upper limit of 2.3 Monte Carlo events gives the indicated upper limit on the $t\bar{t}$ background after cut 4. This is used as the estimate of the total background since $t\bar{t}$ is expected to dominate; b jets can produce a second lepton of the same sign and that lepton has a non-negligable probablility of being well-isolated. The assumption of $t\bar{t}$ dominance is consistent with the results after Cut 3 in Table 9. Two possible backgrounds, $W^{\pm}W^{\pm}$ and $t\bar{t}t\bar{t}$, are probably small but have not been studied.

The $E_{\mathrm{T}}^{\mathrm{miss}}$ distributions after the other cuts are shown in Figure 7. While the rates are small, the S/B ratio is good and the signal is distinctive. The $E_{\mathrm{T}}^{\mathrm{miss}}$ cut was varied and the value in the cuts used here found to be appropriate.

It is clear that the Standard Model same-sign dilepton background is small and is probably dominated by $t\bar{t}$. A data-driven analysis of this background has not yet been done. It is expected that it will be possible to measure the background from processes such as $t \to \ell^+ X$, $\bar{b} \to \mu^+ X$ as a function of the isolation cut and to extrapolate to the cut used here. For $\bar{b} \to e^+ X$, where the e identification cuts impose an implicit isolation cut, it will be necessary to extrapolate from the μ result using Monte Carlo techniques. In the absence of such studies the significance for the same-sign dilepton analysis has been calculated using the 90% upper limit for $t\bar{t}$ given in Table 9 with the standard systematic uncertainty of $\pm 20\%$. This gives the Z_n values listed in the same table. Although the systematic error on the background is uncertain, certainly SU4 and very likely SU1 and SU3 would be observable with a significance greater than 5σ with $1\,\mathrm{fb}^{-1}$.

More work on the same-sign dilepton background, and more generally on estimates of leptons from b and c decays passing isolation cuts, is clearly needed.

5 Three-lepton mode

The trilepton signal from direct gaugino production [14] is perhaps the best search mode for SUSY at the Tevatron [15, 16]. The corresponding search with ATLAS is described elsewhere in this volume [11]. The analyses discussed here are aimed at trilepton production from all sources, not just from direct production. Two approaches have been followed. The first, the 3-leptons + jet selection makes explicit use of a high-p_{T} jet, similar to the 1- and 2-lepton analyses described above. The second, the 3-leptons + $E_{\mathrm{T}}^{\mathrm{miss}}$ selection, relies on track isolation cuts to select prompt leptons and is similar to the exclusive analysis [11]. The 1LEP trigger typically gives an efficiency of $\gtrsim 95\%$ for these modes (see Table 1).

5.1 Three-lepton + jet analysis

The 3-leptons + jet selection requires:

1. At least three leptons with $p_T > 10$ GeV satisfying the usual identification and isolation cuts [1].
2. At least one jet with $p_T > 200$ GeV.

No $E_{\mathrm{T}}^{\mathrm{miss}}$ cut is made, so this analysis could be used even if detector problems seriously degraded the $E_{\mathrm{T}}^{\mathrm{miss}}$ performance. The jet cut is sufficient to suppress the WZ and $W\gamma^*$ backgrounds, so cuts on the invariant mass of opposite-sign same-family dilepton pairs are also not required.

The cut flow for this selection is shown in Table 10. The number of events after all cuts includes the effect of the 1LEP trigger, which, as shown in Table 1, has an efficiency of around 95% for all of the benchmark points considered. The jet cut (Cut 2) particularly reduces the ZW and Zb backgrounds in which the jets tend to be soft. The dominant background after all cuts is $t\bar{t}$, but there is also a small remaining background from WZ. The same table shows the statistical significance $S/\sqrt{B}$ and the significance Z_n including a background uncertainty of 20%. As has already been discussed for the same-sign dilepton selection, the key issue for background determination is the estimation of leptons from $b \to \ell X$ passing the isolation cut in $t\bar{t}$ events. We expect that this could be measured as a function of the isolation cut for μ and then applied to e using Monte Carlo simulation. Given the large S/B in Table 10, even a 100% background uncertainty would yield $Z_n > 5$ for points SU3 and SU4.

Adding a cut on $E_{\mathrm{T}}^{\mathrm{miss}}$ to this analysis was investigated. The surviving background events after the trilepton and jet cuts have a wide range of $E_{\mathrm{T}}^{\mathrm{miss}}$, so a cut to reduce them would also reduce the already rather small signal.

Table 10: The numbers of surviving SUSY and Standard Model events for the benchmark points SU2, SU3 and SU4, as the "3-leptons+jet" inclusive trilepton selection is applied. All numbers are nomalized to 1 fb^{-1} of integrated luminosity.

Sample	Cut 1	Cut 2	S/B	$S/\sqrt{B}$	Z_n
SU2	35	13	1.1	3.7	2.7
SU3	139	94	7.8	27.1	11.5
SU4	1284	312	26.0	90.0	24.4
$t\bar{t}$	455	11	–	–	–
ZZ	59	0	–	–	–
ZW	193	1	–	–	–
WW	3	0	–	–	–
$Z+\gamma$	9	0	–	–	–
Zb	656	0	–	–	–

5.2 Three-lepton + $E_{\mathrm{T}}^{\mathrm{miss}}$ analysis

The 3-leptons $+ E_{\mathrm{T}}^{\mathrm{miss}}$ selection does not require (or veto) jets, so it is sensitive to direct gaugino production as well as to trileptons produced in the decays of squarks and gluinos. The analysis cuts have been somewhat optimized for SU2, for which gaugino pair production dominates. Since the dominant source of trileptons in SUSY includes a decay $\tilde{\chi}_2^0 \to \tilde{\chi}_1^0 \ell^+ \ell^-$, at least one OSSF lepton pair is required among the three leptons.

Table 11: Expected event numbers for the 3-leptons + $E_{\mathrm{T}}^{\mathrm{miss}}$ analysis for 1 fb^{-1} for signal and background processes. The WW and $Z\gamma$ backgrounds are small and so are not listed.

Process	Cuts 1-2	Cut 3	Cut 4	Cut 5
SU1	42.2	33.0	32.6	24.1
SU2	29.8	24.1	21.1	17.6
SU3	130.1	101.2	98.6	63.9
SU4	968.1	691.5	654.3	544.9
SU8.1	10.2	8.0	8.0	5.3
WZ	188.3	166.2	122.5	22.8
ZZ	55.9	46.4	10.3	1.6
Zb	582.5	221	1.3	0
$t\bar{t}$	283.2	59.9	56.6	47.9

The cuts for this analysis are:

1. $N_\ell \geq 3$ leptons with $p_T > 10$ GeV satisfying the usual identification and isolation cuts [1].
2. At least one OSSF dilepton pair with $M > 20$ GeV to suppress low-mass γ^*, J/ψ, Υ, and conversion backgrounds.
3. Lepton track isolation: $p_{T,\mathrm{trk}}^{0.2} < 1$ GeV for muons and < 2 GeV for electrons, where $p_{T,\mathrm{trk}}^{0.2}$ is the maximum p_T of any additional track within a cone $R = 0.2$ around the lepton.

Table 12: Number of signal (S) and background (B) events surviving the 3-leptons $+ E_{\mathrm{T}}^{\mathrm{miss}}$ selection and the corresponding values for $S/\sqrt{B}$ and Z_n. All numbers are normalized to 1 fb^{-1} .

	SU1	SU2	SU3	SU4	SU8
S	24.1	17.6	63.9	544.9	5.3
B			73.5		
$S/\sqrt{B}$	2.8	2.1	7.5	63.5	0.6
Z_n	1.3	1.0	3.5	16.4	0.3

4. $E_{\mathrm{T}}^{\mathrm{miss}} > 30$ GeV.

5. $M < M_Z - 10$ GeV for any OSSF dilepton pair.

Cut 3 provides an additional rejection of leptons from b and c decays beyond the calorimeter isolation cut, while Cut 4 reduces Standard Model backgrounds containing a Z.

The significances $S/\sqrt{B}$ and Z_n for this second analysis are shown in Table 12, where the Z_n significance includes the standard 20% background systematic uncertainty. A detailed study of the performance of the lepton isolation cuts is needed to understand the uncertainty on the $t\bar{t}$ background in particular. Since this analysis does not require jets, one might hope that it would be sensitive to the dominant gaugino pair production for SU2, but only SU4 gives a signal with $Z_n > 5$ for 1 fb^{-1}. For all of the benchmark points studied the 3-leptons + jet analysis is more sensitive than the 3-leptons $+ E_{\mathrm{T}}^{\mathrm{miss}}$ one.

6 Tau mode

SUSY models generically violate $e/\mu/\tau$ universality; τ decays can even be dominant, especially for $\tan\beta \gg 1$. Hence it is worthwhile to look for signatures involving hadronic τ decays even though the fake background from jets is much larger than that for e or μ. Leptonic τ decays are indistinguishable from prompt leptons and are already included in the previous analyses.

The cuts used in this analysis are:

1. At least four jets with $p_T > 50$ GeV and at least one with $p_T > 100$ GeV.

2. $E_{\mathrm{T}}^{\mathrm{miss}} > 100$ GeV.

3. $\Delta\phi(j_i, E_{\mathrm{T}}^{\mathrm{miss}}) > 0.2$ for each of the three leading jets j_i, $i = 0,1,2$.

4. No isolated leptons using the standard cuts [1].

5. At least one τ with $p_T > 40$ GeV and $|\eta| < 2.5$ reconstructed by the high p_T τ algorithm [17] with a likelihood, $L > 4$.

6. $E_{\mathrm{T}}^{\mathrm{miss}} > 0.2 M_{\mathrm{eff}}$.

7. $M_T > 100$ GeV, where M_T is calculated using the visible momentum of the hardest τ and $E_{\mathrm{T}}^{\mathrm{miss}}$.

Cuts 1, 2, and 6 are standard. Cut 3 requires a large $\Delta\phi$ between $E_{\mathrm{T}}^{\mathrm{miss}}$ and the leading jets, thus reducing the background both from mismeasured jets and from b and c decays. Cut 4 makes this analysis disjoint from the 1, 2, and 3-lepton analyses described above. There is still overlap with the 0-lepton analysis described in Section 2. Cut 5 defines the τ sample; these cuts give an efficiency of $\sim 50\%$ with a purity

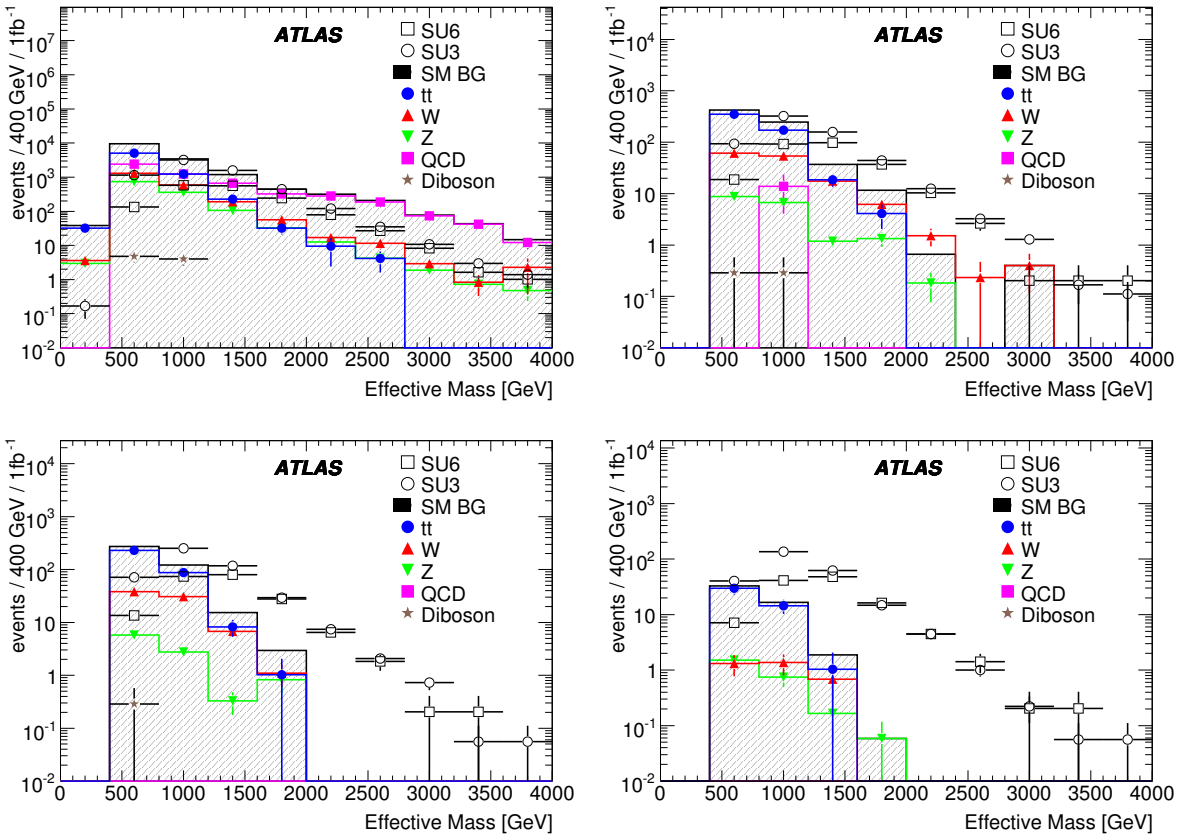

Figure 8: The M_{eff} distributions for SUSY signals and Standard Model backgrounds in the τ analysis after Cuts 4, 5, 6, and 7.

Table 13: The number of signal (S) and background (B) events after tau selection and corresponding values of significance, normalised to 1 fb^{-1}.

Sample	S	B	S/B	$S/\sqrt{B}$	Z_n
SU3	259	51	5.1	36.3	12
SU6	119	51	2.3	16.7	6.8

of $\sim 80\%$ for the SU3 sample. Finally, if the $E_{\text{T}}^{\text{miss}}$ comes from one $W \to \tau\nu$ decay, then M_T used in Cut 7 should satisfy $M_T < m_W$. The applied cuts are a superset of the basic cuts for the inclusive 4-jet 0-lepton analysis, which does not employ a τ veto and therefore the events selected for this analysis will have an almost complete overlap with the ones selected in the analysis described in the corresponding section. For the same reason, the efficiency of the j70xE70 trigger is expected to be between 97% and $\sim$100% for all the benchmark points, as was the case for the inclusive multi-jet analysis.

The effect of these cuts is indicated graphically in Figure 8. The requirement of a reconstructed τ (Cut 5) eliminates the QCD background. After the M_T cut the S/B ratio is high. The resulting signal, background, and significance for points SU3 and SU6 are given in Table 13 assuming the usual 20% systematic uncertainty for the background, which is dominated by $t\bar{t}$ with some contribution from $W+$ jets.

The data-driven uncertainty on τ SUSY backgrounds has not yet been studied. Clearly τ reconstruc-

tion is difficult. However, it should be possible to simulate real τ backgrounds by selecting backgrounds with reconstructed e and μ and replacing the leptons with simulated τ decays. Fake backgrounds can be similarly determined using reconstructed events combined with the measured jet $\rightarrow \tau$ fake rate. If the resulting uncertainty on the background is about 20%, as is assumed in Table 13, then both points SU3 and SU6 would be observable in the τ mode.

7 b-jet mode

SUSY signals are typically rich in b quarks because the $\tilde{b}$ and $\tilde{t}$ tend to be lighter than first- and second-generation squarks and because Higgsino couplings enhance heavy flavour production. In the benchmark points studied the fractions of events containing b jets range from 14.4% for SU2 to 72.8% for SU4. In QCD events b quarks typically occur at the percent level. Thus, requiring a b quark suppresses the QCD background, which may be difficult to control, just as requiring an e or μ does.

In this section an analysis of signatures with b jets is performed for SUSY points SU1, SU3, SU4 and SU6 using full simulation both for the signal and for the Standard Model backgrounds. Isolated leptons may also be present, and all channels with and without leptons are summed. SUSY processes almost always will give $b\bar{b}$ pairs, and this is taken into account. No equivalent analysis was performed in the Physics TDR.

The cuts used in this analysis are as follows:

1. At least 4 jets in the event with $p_{\mathrm{T}} > 50$ GeV.
2. Leading jet $p_{\mathrm{T}} > 100$ GeV.
3. Missing transverse energy, $E_{\mathrm{T}}^{\mathrm{miss}} > 100$ GeV.
4. Missing transverse energy, $E_{\mathrm{T}}^{\mathrm{miss}} > 0.2 M_{\mathrm{eff}}$.
5. Transverse sphericity, $S_T > 0.2$.
6. At least 2 jets are tagged as b jets, as described below.
7. $M_{\mathrm{eff}} > 600$, 800, or 1000 GeV.

Note that Cuts 1–3 are also used in Monte Carlo generator filters for some of the background samples. Cut 7 is used to optimize the signal-to-background ratio in the selected events.

Jets with $p_T > 20$ GeV are selected as b jets using the default tagging algorithm based on the 3-dimensional impact parameter and secondary vertex detection [18] with a cut weight > 6.75, giving a nominal efficiency of 60%. Above about $p_T = 100$ GeV both the efficiency and the light-jet rejection decrease as discussed in the introductory SUSY note [1] and references therein. Naively one would expect that the increase of the B decay length with $\gamma = E_B/M_B \gg 1$ would offset the $1/\gamma$ decrease of the angles since the multiple scattering angular errors also decrease similarly. There is also a substantial dependence of b tagging on the η of the jet. Many of the b jets in SUSY events have high p_T: the typical p_T of the leading jet in SU3 is about 300 GeV, for which the light-jet rejection during b tagging is $\mathcal{O}(100)$.

Events with zero or more leptons and at least two tagged b jets were combined in a single inclusive analysis. Inevitably this means that there is overlap with the analyses in Sections 2–5. The cut flow is shown in Table 14. After Cut 6 ($N_b \geq 2$) the $t\bar{t}$ background is dominant, as one might expect, but the QCD background remains substantial. The b-tagging performance at high p_T is clearly an important issue for this analysis. As the applied cuts are a superset of the basic cuts for the inclusive 4-jet analyses,

Table 14: Number of events surviving selection cuts as defined in the text for the inclusive search with b jets normalized to 1fb^{-1} using NLO cross-sections. The results are shown for three different values of the M_{eff} cut (Cut 7).

Sample	Cuts 1–3	Cut 4	Cut5	Cut 6	Cut 7		
					600 GeV	800 GeV	1000 GeV
SU1	3469	2806	1994	456	442	375	263
SU2	608	358	299	170	166	141	87
SU3	9357	7279	5474	1158	1086	818	425
SU4	79761	56697	45661	16478	10204	3186	926
SU6	2557	2049	1467	505	495	436	340
$t\bar{t}$	12864	8273	6117	2182	836	215	61
QCD	29435	7402	5171	740	259	79	5
$W+$jets	4068	2309	1600	23	16	7	2
$Z+$jets	1249	680	432	5	3	1	1
Diboson	22	13	8	2	1	0	0
B_{SM}	47527	18676	13328	2950	1115	303	69

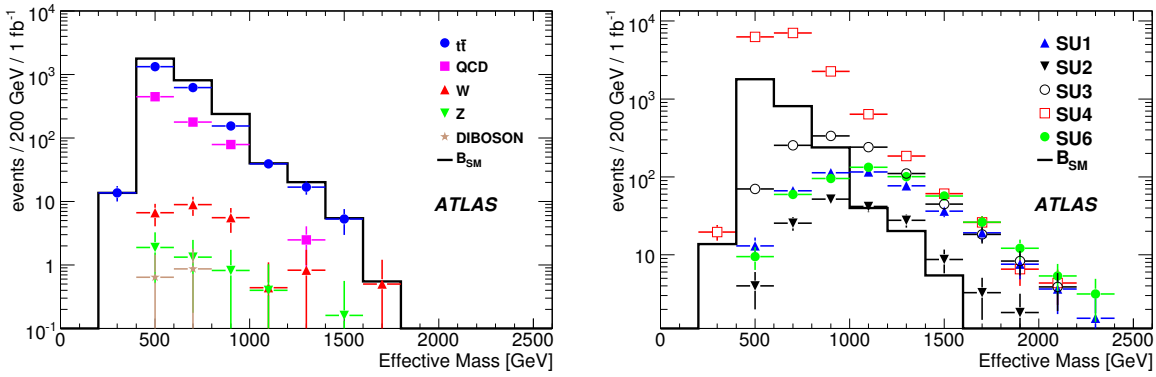

Figure 9: M_{eff} distributions for b-jet analysis. Left: Standard Model backgrounds. Right: SUSY signals with total background.

the efficiency of the j70xE70 trigger is, as quoted in the corresponding section, between 97% and ∼100% for all the considered benchmark points.

To calculate the significance in this channel an uncertainty of 50% for the QCD background and 20% for the other backgrounds is assumed for 1 fb^{-1}. The uncertainty on the b-tagging efficiency of 60% is 5% [2, 18]. This is assumed to be included in the $t\bar{t}$ uncertainty and is ignored for the other, smaller backgrounds.

The hardest effective mass cut, $M_{\text{eff}} > 1000$ GeV, was found to be the most effective, so only results for it are shown here. The resulting significances, Z_n, including the above systematic effects, are shown in Table 15, for two luminosities: 0.1 and fb^{-1}, where the same systematic uncertainty is assumed to be the same for both luminosities. All background uncertainties are added linearly. The low-mass point SU4 and perhaps also SU3 could be discovered using this analysis with only 0.1 fb^{-1} assuming that the background could be understood adequately. All points except SU2 could be discovered with 1 fb^{-1}, for

Table 15: S/B ratio and signal significance Z_n including systematic effects for the b-jet analysis with $0.1\,\text{fb}^{-1}$ and $1\,\text{fb}^{-1}$ with $M_{\text{eff}} > 1000$ GeV.

	S/B	Z_n for $0.1\,\text{fb}^{-1}$	Z_n for $1\,\text{fb}^{-1}$
SU1	3.8	6.0	9.3
SU2	1.3	2.3	5.0
SU3	6.2	7.5	13.0
SU4	13.4	12.6	21.7
SU6	4.9	7.1	11.2

which the background uncertainties are realistic. This analysis seems to be particularly useful compared to some other analyses for point SU6.

8 Scans and optimization

The SUSY points studied so far were chosen to give a variety of signatures, but there is no reason to think that they are representative of what might be found at the LHC. This section uses scans over the parameters of several models for SUSY breaking – all with R parity conservation – in order to sample a wider range of possibilities. The goal is to develop one or more search strategies covering as wide a subset of the scanned models as possible. Since each scan includes hundreds of points, this section must rely on ATLFAST [19], the fast parameterized simulation of the ATLAS detector.

Data-driven methods [2,3] will be used to determine the Standard Model backgrounds to the possible SUSY signatures. For $1\,\text{fb}^{-1}$ the estimated errors [2, 3] are typically 50% for QCD jets and 20% for the W, Z, and t backgrounds. Several approaches were considered to look for an excess above a cut on M_{eff} or $E_{\text{T}}^{\text{miss}}$ after basic jet and lepton selections. The significance is corrected for multiple cuts as described in Section 1.2. Results are shown here only for the M_{eff} cut, that yielded best performance. A multivariate optimization using TMVA [20] gave a minor improvement with the available Monte Carlo statistics. This and other cut procedures are still being studied.

The analyses described above in this note have used signal and background cross-sections normalized to next-to-leading-order calculations [1]. This was impractical for scans over many points, each involving many subprocesses. The goal here is not to determine the exact limit or exclusion value but rather to test whether the proposed approaches work for a wide range of models. It was therefore decided to normalize the signal cross-sections for all scans to the leading-order HERWIG values but to use next-to-leading-order normalizations for the backgrounds. Since next-to-leading-order corrections generally increase cross-sections, the resulting reach estimates are conservative.

8.1 SUSY signal samples

It is impossible to scan the 105-dimensional parameter space of the MSSM or even the 19 dimensional subspace with flavour and CP conservation and degeneracy of the first two generations. Hence a number of SUSY-breaking models with many fewer parameters were used.

Several of these scans (e.g. the first two mSUGRA scans listed below) ignore dark matter and other existing constraints. Of course any true theory must obey such constraints. It is possible, however, to modify the SUSY breaking model to satisfy the constraints while keeping the basic phenomenology unchanged. One such example, the non-universal-Higgs model (NUHM), is discussed below. Since there is no unique model of SUSY-breaking, all these scans should be viewed only as possible patterns of LHC

signatures, not as complete theories.

mSUGRA fixed grid, $\tan\beta = 10$, $A_0 = 0$, $\mu > 0$: A 25×25 grid was made varying m_0 from 60 GeV to 2940 GeV in 25 steps of 120 GeV, and $m_{1/2}$ from 30 GeV to 1470 GeV in 25 steps of 60 GeV. SUSY spectra were generated using ISAJET 7.75 [21] with a top quark mass of 175 GeV. Out of the 625 possible points, a spectrum could be successfully generated for 600; the other 25 failed for theoretical reasons. For each good point 20k events were produced using ATLFAST. Constraints other than from direct searches were ignored. While constraints such as the dark-matter relic density constrain specific SUSY-breaking models such as mSUGRA, they are much less restrictive for generic models.

mSUGRA fixed grid: $\tan\beta = 50$, $A_0 = 0$, $\mu < 0$: Large $\tan\beta$ increases the mixing of $\tilde{b}_{L,R}$ and $\tilde{\tau}_{L,R}$, leading to enhanced b and τ production. A grid of 25×25 points with was generated with m_0 varied from 200 to 3000 GeV in steps of 200 GeV and with $m_{1/2}$ varied from 100 to 1500 GeV in steps of 100 GeV. The top mass was fixed at 175 GeV. Constraints other than from direct searches were again ignored.

mSUGRA random grid with constraints: In this sample all mSUGRA parameters were varied in two regions[3)] previously found [22] to be compatible with dark-matter and other constraints with $\mu > 0$ and $m_t = 175$ GeV.

The mSUGRA parameters were chosen randomly (with $\mu > 0$) and their properties calculated using ISAJET 7.75. All selected points satisfy the LEP Higgs mass limit, $m_h > 114.4$ GeV [23]; the WMAP total dark matter limit, $\Omega h^2 < 0.14$ [24]; within 3σ the branching ratio limits $B(b \to s\gamma) = (3.55 \pm 0.26) \times 10^{-4}$ [25] within 3σ and $B(B_s \to \mu^+\mu-) < 1.5 \cdot 10^{-7}$ [26]; and with δa_μ less than the 3σ upper limit from the muon anomalous magnetic moment measurement $a_\mu = (11659208 \pm 6) \times 10^{-10}$ [27].

GMSB grid: $M_{\rm mess} = 500$ TeV, $N_{\rm mess} = 5$, $C_{\rm grav} = 1$: With $N_{\rm mess} = 5$ the NLSP is a slepton which decays promptly to leptons or τ's. A fixed grid was made varying Λ was varied from 10 TeV to 80 TeV in steps of 10 TeV and $\tan\beta$ from 5 to 40 in steps of 5.

NUHM grid: The NUHM model is similar to the mSUGRA model but does not assume that the Higgs masses unify with the squark and slepton ones at the GUT scale. This allows more gaugino/Higgsino mixing at the weak scale and so relaxes the mSUGRA dark matter constraints. The scan uses a step size of 100 GeV in both m_0 and $m_{1/2}$. For each point the values of μ and M_A at the weak scale are adjusted to give acceptable cold dark matter.

8.2 ATLFAST corrections

ATLFAST is a fast parameterized simulation of the ATLAS detector. The version used here is rather idealized. Corrections to the efficiency for e reconstruction were applied as a function of p_T and η. An example of the effect of these corrections is shown in Figure 10. In addition, the ATLFAST algorithm finding reconstructed cone jets was missing the split-merge step, so jets matched to the same truth jet were combined. With these corrections the ATLFAST and full simulations agree reasonably well. All results shown here use ATLFAST with these corrections.

[3)] The parameters are varied within $\{0 < m_0 < 2$ TeV, $0.5 < m_{1/2} < 1.3$ TeV, $-0.34 < A_0 < 2.4$ TeV, $39 < \tan\beta < 55\}$ and $\{1 < m_0 < 3$ TeV , $m_{1/2} < 0.5$ TeV , $-2.0 < A_0 < 2.0$ TeV, $20 < \tan\beta < 55\}$

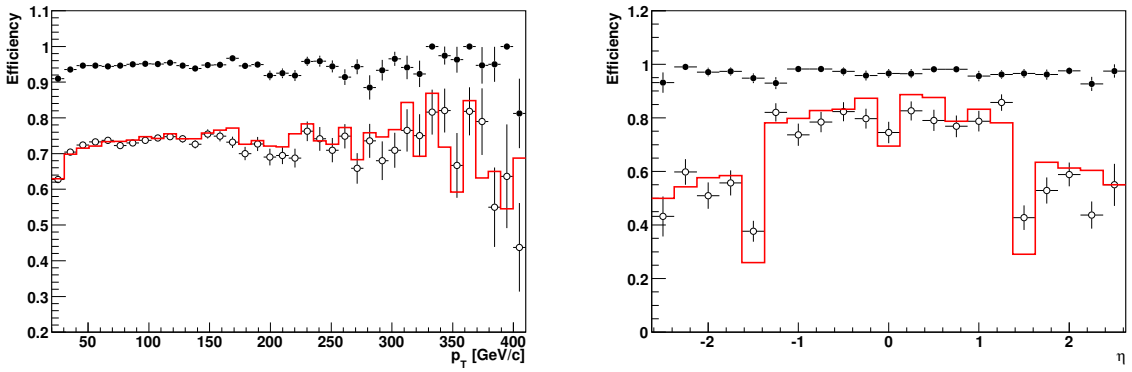

Figure 10: Efficiencies for electrons as a function of p_T for the SU3 sample (left) and η for the ALPGEN sample $Z \rightarrow ee$ (right). The solid red line corresponds to the Geant 4 simulation, the solid circles to uncorrected ATLFAST, and the open circles to the corrected version of ATLFAST used for the reach analyses.

8.3 Discovery reach

The reach plots in this subsection are all based on analyses that require a certain number of jets and leptons (e or μ) and then find an optimal $M_{\rm eff}$ cut (in steps of 400 GeV) to maximize the significance Z_n corrected for multiple cuts of the signal over the Standard Model background, using background errors estimated from studies of data-driven methods [2,3]. Not all modes were studied because of limited time or Monte Carlo statistics.

The analysis most similar to that in the Physics TDR [10], requires four jets with $p_T > \{100, 50, 50, 50\}$ GeV and $E_{\rm T}^{\rm miss} > \max(100\ {\rm GeV}, 0.2M_{\rm eff})$. The 5σ discovery reach for the analyses reqiring zero, one, or two opposite-sign leptons for mSUGRA with $\tan\beta = 10$ are shown in Figure 11. The plot also shows the trilepton reach with just one jet. The 0-lepton mode has the best estimated reach, close to 1.5 TeV for the smaller of $m_{\tilde{g}}$ and $m_{\tilde{q}}$. The 1-lepton estimated reach is somewhat less, but it is more robust against QCD backgrounds which might result from detector problems. Figure 11 also shows that the reach for $\tan\beta = 50$ is similar for the zero- and one-lepton channels. Despite the enhanced τ decays for $\tan\beta \gg 1$, the one-τ reach is slightly worse than the reach for zero and one leptons. This reflects the lower efficiency and purity for τ reconstruction. Compared to $\tau + 4$ jets, the reach for $\tau + 3$ jets is slightly better, while $\tau + 2$ jets is about the same. The curves for the $\tau + 2$-jet and the $\tau + 3$-jet analyses are not shown.

Requiring four jets is not necessarily the best choice. The 5σ reach contours for the 0-lepton plus $E_{\rm T}^{\rm miss}$ and the 1-lepton plus $E_{\rm T}^{\rm miss}$ analyses for various jet multiplicities are shown in Figure 12, again for the $\tan\beta = 10$ mSUGRA scan. For the 0-lepton mode the choice of four jets seems best, while for the 1-lepton mode the 2-jet, 3-jet and 4-jet reaches are all comparable. The reaches (not shown here) for the opposite-sign dilepton plus $E_{\rm T}^{\rm miss}$ signature requiring at least 2, 3, or 4 jets are comparable and in all cases are less than the reaches for the 0-lepton and 1-lepton modes. Observing a signal in multiple channels would provide further confidence that the observed excesses were evidence for new physics.

The mSUGRA "random" scan with low-energy constraints samples only a limited range of parameters and hence of gluino and squark masses. The results of this scan are shown as a scatter plot of points in Figure 13 compared to those for the mSUGRA scans. The reach for those mSUGRA points which are compatible with low-energy constraints is comparable to that for generic points. This is not surprising given that the SUSY production cross-sections are mainly controlled by the gluino and squark masses, but it adds support to the approach used in this section.

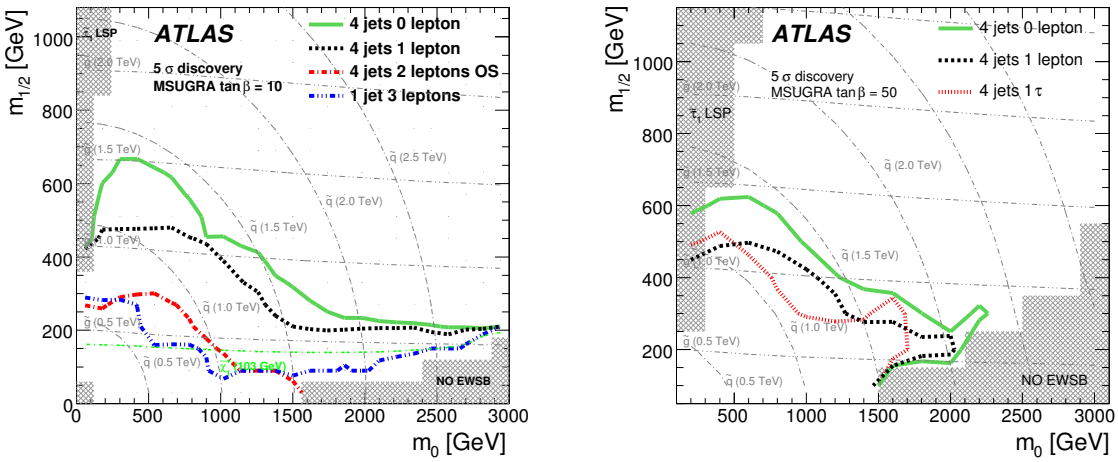

Figure 11: The 1 fb^{-1} 5σ reach contours for the 4-jet plus $E_{\mathrm{T}}^{\mathrm{miss}}$ analyses with various lepton requirements for mSUGRA as a function of m_0 and $m_{1/2}$. Left: $\tan\beta = 10$. Right: $\tan\beta = 50$. The horizontal and curved grey lines indicate gluino and squark mass contours respectively in steps of 500 GeV.

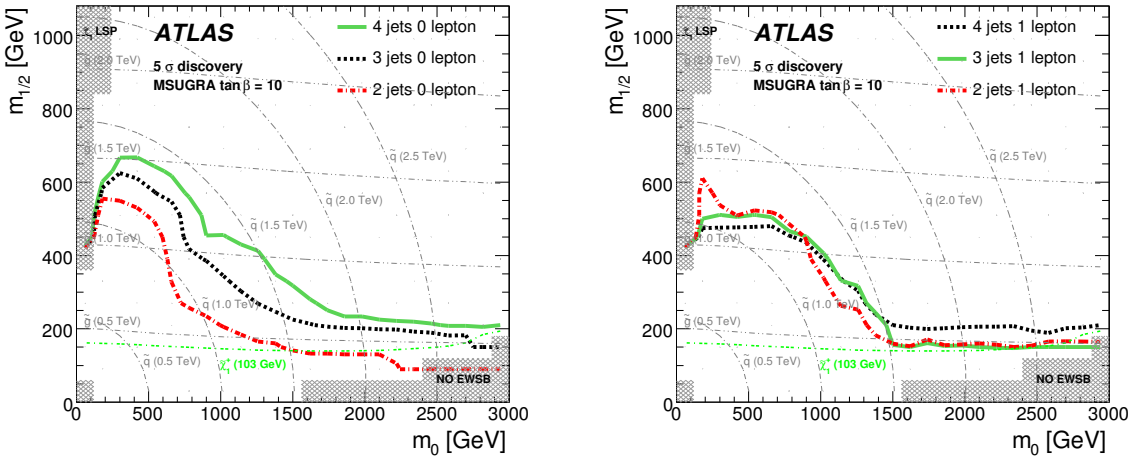

Figure 12: The 1 fb^{-1} 5σ reach contours for the 0-lepton and 1-lepton plus $E_{\mathrm{T}}^{\mathrm{miss}}$ analyses with various jet requirements as a function of m_0 and $m_{1/2}$ for the $\tan\beta = 10$ mSUGRA scan. The horizontal and curved grey lines indicate the gluino and squark masses respectively in steps of 500 GeV.

The mSUGRA model is only one possible mechanism for SUSY breaking. The non-universal-Higgs model has qualitatively similar phenomenology but different patterns of masses and decay modes. The reach plots with four jets, zero or one leptons, and $E_{\mathrm{T}}^{\mathrm{miss}}$ for the NUHM are shown in Figure 14. The reach with zero and one leptons is virtually identical to that for mSUGRA. This is as expected: adding some Higgsino mixing allows $\tilde{\chi}_1^0$ annihilation but has a minor effect on the other decays.

Another alternative often considered, Anomaly Mediated SUSY Breaking (AMSB), is not examined here. Previous studies [28] have found an overall reach comparable to mSUGRA with similar assumptions. The reach in the one-lepton modes is less because the lightest chargino is almost degenerate with the LSP and so does not give visible leptons.

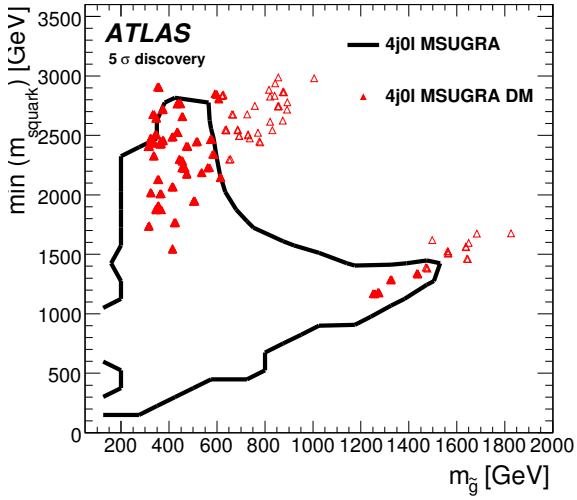

Figure 13: Reach for the "random with constraints" mSUGRA scan plotted in the $m_{\tilde{g}}, m_{\tilde{q}}$ plane. Solid triangles represent points which are observable ($Z_n > 5$) with $1\,\text{fb}^{-1}$, while open triangles show points which are not.

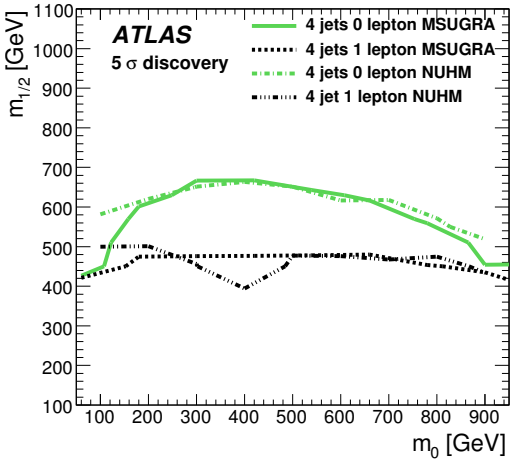

Figure 14: The 1 fb^{-1} reach for NUHM models with 4 jets, 0 or 1 leptons, and $E_{\text{T}}^{\text{miss}}$. The masses for NUHM are similar to those shown in Figure 11.

The models considered in the GMSB scan all have at least two leptons or τ's at the Monte Carlo generator level, so the signatures are easier to distinguish from Standard Model backgrounds. The reach plots for this scan are shown in Figure 15. The reach for three leptons is significantly better than for two leptons and extends well beyond 2 TeV for gluinos for large $\tan\beta$ and is close to 2 TeV for all $\tan\beta$. Special signatures that can result from GMSB models are discussed elsewhere in this volume [4].

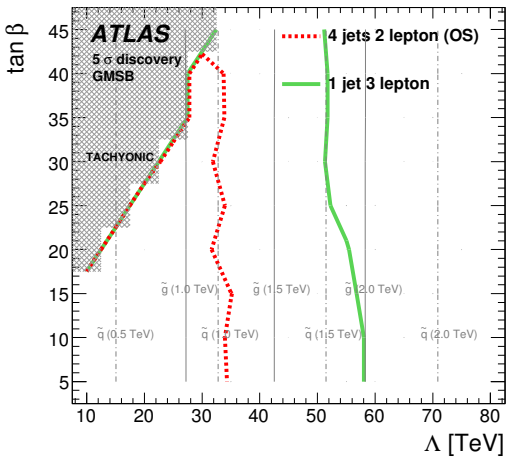

Figure 15: The 1 fb^{-1} 5σ reach contours of the 2-lepton and 3-lepton analyses for the GMSB scan. The vertical solid and dashed grey lines indicate the gluino and squark masses respectively in steps of 500 GeV.

8.4 Summary

The results of the scans presented in this section together with the full simulation analyses presented earlier indicate that ATLAS should discover signals for *R*-parity conserving SUSY with gluino and squark masses less than $\mathcal{O}(1\text{ TeV})$ after having accumulated and understood an integrated luminosity of about 1 fb^{-1}. For favorable models the mass reach could be greater. The luminosity required to discover a given SUSY scenario is greater than that estimated previously [29]. The main differences in this analysis are that the uncertainty in the background (derived from data-driven methods) is taken into account and that the signal and background simulations are more realistic. Given the admittedly qualitative naturalness arguments about SUSY masses, it is plausible that SUSY could be found with 1 fb^{-1} if it exists at the TeV scale. Conversely, if SUSY is not found with 1 fb^{-1}, it might still eventually be discovered at the LHC, but it will be difficult to study in detail.

References

[1] ATLAS Collaboration, *Supersymmetry searches with ATLAS*, this volume.

[2] ATLAS Collaboration, *Data-driven determinations of W, Z, and top background to supersymmetry*, this volume.

[3] ATLAS Collaboration, *Estimation of QCD backgrounds to searches for Supersymmetry*, this volume.

[4] ATLAS Collaboration, *Supersymmetry signatures with high p_T photons or long-lived heavy particles*, this volume.

[5] ATLAS Collaboration, *ATLAS High-Level Trigger, Data Acquisition and Controls Technical Design Report*, ATLAS TDR-016 (2003).

[6] ATLAS Collaboration, *The ATLAS trigger for early running*, this volume.

[7] R.D. Cousins and V.L. Highland, Nucl. Instrum. Meth. **A320** (1992) 331–335.

[8] J. T. Linnemann, Measures of significance in HEP and astrophysics, 2003.

[9] R. Brun, and F. Rademakers, Nucl. Instrum. Meth. **A389** (1997) 81–86.

[10] ATLAS Collaboration, *ATLAS detector and physics performance. Technical design report* Vol. 2, CERN-LHCC-99-15 (1999).

[11] ATLAS Collaboration, *Multi-lepton Supersymmetry searches*, this volume.

[12] C. Lester, D. Summers, Phys. Lett. **B463** (1999) 99.

[13] A.J. Barr, C.G. Lester, P. Stephens, J. Phys. G. **29** (2003) 2343.

[14] H. Baer, K. Hagiwara and X. Tata, Phys. Rev. Lett **57**, 294 (1986) and Phys. Rev. D**35**, 1598 (1987); R. Arnowitt and P. Nath, Mod. Phys. Lett. **A2**, 331 (1987); R. Barbieri, F. Caravaglios, M. Frigeni and M. Mangano, Nucl. Phys. **B367**, 28 (1991); H. Baer and X. Tata, Phys. Rev. D**47**, 2739 (1993); J. Lopez, D. Nanopoulos, X. Wang and A. Zichichi, Phys. Rev. D**48**, 2062 (1993); H. Baer, C. Kao and X. Tata, Phys. Rev. D**48**, 5175 (1993); S. Mrenna, G. Kane, G. D. Kribs and J. D. Wells, Phys. Rev. D**53**, q1168 (1996)..

[15] CDF Collaboration, CDF/PUB/EXOTIC,PUBLIC/9176, http://www-cdf.fnal.gov/physics /exotic/r2a/20080110.trilepton_dube/cdf9176.pdf.

[16] D0 Collaboration, D0 Note 5348-Conf, http://www-d0.fnal.gov/Run2Physics/WWW/results/prelim/NP/N52/N52.pdf.

[17] ATLAS Collaboration, *Reconstruction and identification of hadronic tau decays with ATLAS*, this volume.

[18] ATLAS Collaboration, *Vertexing for b-tagging*, this volume.

[19] Richter-Was, Elzbieta and Froidevaux, Daniel and Poggioli, Luc, *ATLFAST 2.0 a fast simulation package for ATLAS* Atlas Note ATL-PHYS-98-131.

[20] A. Hocker *et al.*, *TMVA: Toolkit for multivariate data analysis*, physics/0703039, 2007.

[21] F. Paige, S. Protopopescu, H. Baer and X. Tata, *ISAJET 7.69: A Monte Carlo event generator for p p, anti-p p, and e+ e- reactions* hep-ph/0312045, 2003.

[22] R.R. de Austri, R. Trotta and L. Roszkowski, JHEP **05** (2006) 002.

[23] R. Barate *et al.*, Phys. Lett. **B565** (2003) 61–75.

[24] D. Spergel *et al.*, Astrophys. J. Suppl. **170** (2007) 377.

[25] E. Barberio *et al.*, *Averages of b-hadron properties at the end of 2006*. arXiv:0704.3575 [hep-ex], 2007.

[26] A. Abulencia *et al.* (CDF Collaboration), Phys. Rev. Lett. **94** (2005) 221805.

[27] G.W. Bennett *et al.*, Phys. Rev. Lett. **92** (2004) 161802.

[28] A.J. Barr, C.G. Lester, M.A. Parker, B.C. Allanach and P. Richardson, JHEP **03** (2003) 045.

[29] D.R. Tovey, Eur. Phys. J. Direct **C4** (2002) N4.